

?

# Self-Optimizing Control of a LNG Liquefaction Plant

Adriaen Verheyleweghen, Johannes Jäschke

*Department of Chemical Engineering, Norwegian Univ. of Science and technology,  
Trondheim, NO-7491 (e-mail: verheyle@ntnu.no, jaschke@ntnu.no).*

---

## Abstract

The application of self-optimizing control theory to a two-stage refrigeration cycle was investigated. Defining the cost function as the economical trade-off between the power consumption and the evaporator outlet temperatures, it was found that the optimal point of operation leaves two unconstrained degrees of freedom for implementing a self-optimizing control structure. We consider two cases: (1) where the self-optimizing control structure is designed to optimally reject only physical process disturbances, and (2) where the control structure in addition handles changes in the economic parameters of the cost function. The control structure is able to keep the process close to optimal despite disturbances and changes in the product prices, and thus making a supervisory real-time optimization (RTO) layer unnecessary.

*Keywords:* Self-optimizing control; refrigeration cycle; optimal control;

---

## 1. Introduction

**Keep as is, say a few words about MR vs. Cascade**

Recently there has been an increased focus on improving energy efficiency in industry. Especially in large processes such as in the petrochemical industry there are substantial potentials for savings due to the large power consumption. Multi-stage refrigeration cycles are large consumers of energy, so their optimal operation is an important topic of research.

In the presence of disturbances, implementation errors and changing operating conditions, the optimal operation of a process plant becomes non-trivial. One method for achieving optimal operation at all times is "on-line optimization" [7]. Unfortunately, this method can be quite costly since it is often based on the optimization of a control trajectory over a prediction horizon. Depending on the complexity of the model, this dynamic optimization can be very computationally intensive. Model based control of refrigeration cycles was investigated further by [16] and [19]. A lot of research has been done on the field of economic model predictive control for supermarket refrigeration systems, see for instance [17, 21, 9] and the therein included references. The disadvantage of a model

predictive control approach is that it requires a good model of the process, and that the computation time might be prohibitive.

A much simpler approach is to use a simple control structure to keep a carefully selected controlled variable at a constant setpoint. This concept was introduced by [22] and coined "self-optimizing control". More precisely: More precisely: "Self-optimizing control is when we can achieve an acceptable loss with constant setpoint values for the controlled variables (without the need to reoptimize when disturbances occur)." [22]

The self-optimizing controlled variables are often selected as either single measurements or linear combinations of measurements, which are usually controlled by simple PI or PID controllers.

Optimal operation of simple refrigeration cycles was studied by [12, 13], who propose to use a feedback controller to keep a linear combination of two measurements, the high pressure and a temperature, constant. They determine the optimal combination of the measurements using the extended null space method [1]. [18] proposes a similar strategy based on using a cascade formulation with the outer loop calculating the setpoint for the condenser pressure slave controller. Both Jensen and Larsen consider different variations of a single-stage layout.

In this paper we design a self-optimizing control structure for a two-stage refrigeration cycle to ensure the optimal operation. It thereby generalizes the results suggested by [13] by including all plant measurements rather than just pressure and temperature measurements. We also apply a branch and bound algorithm [14] to find the optimal subset of measurements that minimize the loss. Finally, we show how self-optimizing control can be used to ensure optimal operation when the cost parameters are not constant over time.

In the following section, self-optimizing control theory will be presented. In Section 3.1, the model of the two-stage refrigeration cycle will be presented. Two variations of the same case were studied. The first case resulted in a self-optimizing control structure with five plant measurements. The second case resulted in a self-optimizing control structure with measurements of the economic parameters from the cost function in addition to the five plant measurements. Results from the optimizations will be presented in Section 3.1 and Section 4. Finally, the conclusion is presented in Section 5.

## 2. Self-optimizing control

Keep as is

The controlled variable which is a linear combination of measurements is designed such that it satisfies

$$\mathbf{c} = \mathbf{H} \cdot \mathbf{y} \quad (1)$$

$\mathbf{H}$  is known as the selection matrix.  $\mathbf{c}$  is chosen such that the loss  $L$  is minimized

$$\begin{aligned} \min_{\mathbf{u}, \mathbf{c}} L &= J(\mathbf{u}, \mathbf{c}) - J^{\text{opt}}(\mathbf{d}) \\ \text{s.t.} \quad \mathbf{g}(\mathbf{u}, \mathbf{y}) &\leq \mathbf{0} \end{aligned} \quad (2)$$

The optimization is subject to equality- and inequality constraints on the decision variables. Active constraints must be controlled to avoid a large back-off from the optimal solution [25]

The remaining unconstrained problem from Equation 2 is approximated by a Taylor expansion truncated after three terms, yielding

$$L \approx \frac{1}{2} (\mathbf{u} - \mathbf{u}^{\text{opt}})^\top \cdot \mathbf{J}_{\mathbf{uu}} \cdot (\mathbf{u} - \mathbf{u}^{\text{opt}}) \quad (3)$$

It has been used that the gradient  $J_u$  is zero at the optimum.

#### *Exact local method*

A commonly used method to obtain the selection matrix  $\mathbf{H}$  is called the exact local method. Assume that the cost function can be approximated by a local Taylor expansion around the nominal point. It is then shown by [15] that the average loss from Equation 3 for all linear combinations of implementation errors and disturbances is given by

$$L_{\text{avg}} = \frac{1}{2} \|[\mathbf{M}_{\mathbf{d}} \quad \mathbf{M}_{\mathbf{ny}}]\|_F^2 \quad (4)$$

where the Frobenius norm is signified by the subscript  $F$ .

It can be shown that the normed term from Equation 4 can be written as

$$[\mathbf{M}_{\mathbf{d}} \quad \mathbf{M}_{\mathbf{ny}}] = \mathbf{J}_{\mathbf{uu}}^{1/2} (\mathbf{H}\mathbf{G}^y)^{-1} \mathbf{H}\mathbf{Y} \quad (5)$$

where

$$\mathbf{Y} = [\mathbf{F}\mathbf{W}_{\mathbf{d}} \quad \mathbf{W}_{\mathbf{ny}}] \quad (6)$$

The sensitivity matrix is defined as  $\mathbf{F} = \frac{\Delta \mathbf{y}^{\text{opt}}}{\Delta \mathbf{d}}$ . It is assumed that both the disturbances and the measurement errors follow a Gaussian distribution.  $\mathbf{W}_{\mathbf{ny}}$  and  $\mathbf{W}_{\mathbf{d}}$  are diagonal matrices containing the variances of the measurement errors and the disturbances, respectively.

Subsequently, the selection matrix that minimizes Equation 4 is given by the following expression.

$$\min_{\mathbf{H}} = \left\| \mathbf{J}_{\mathbf{uu}}^{1/2} (\mathbf{H}\mathbf{G}^y)^{-1} \mathbf{H}\mathbf{Y} \right\|_F \quad (7)$$

An analytical solution of  $\mathbf{H}$  which satisfies Equation 7 is: [2]

$$\mathbf{H}^\top = (\mathbf{Y}\mathbf{Y}^\top)^{-1} \mathbf{G}^y \left( \mathbf{G}^{y\top} (\mathbf{Y}\mathbf{Y}^\top)^{-1} \mathbf{G}^y \right)^{-1} \mathbf{J}_{\mathbf{uu}}^{1/2} \quad (8)$$

It can be shown that Equation 8 can be simplified to: [26]

$$\tilde{\mathbf{H}}^\top = (\mathbf{Y}\mathbf{Y}^\top)^{-1} \mathbf{G}^y \quad (9)$$

### 3. Case one - Simplified process with single-stage compression

#### 3.1. Process description

The process studied in this work is based on the ConocoPhillips LNG refrigeration plant. A cascaded refrigeration plant consists of multiple closed loops which exchange heat with each other. The advantage of such a design is that the mean temperature difference between the hot and cold sides can be decreased, thus resulting in lower energy consumption. This particular plant has three refrigerant loops; propane, ethane and methane.

two-stage refrigeration cycle described by [5]. A full description of the model used in this work can be found in [24]. The process is based on a similar refrigeration cycle that is currently being operated in a petrochemical plant. A figure of the process can be seen in Figure 1.

The evaporators are flooded with integrated tanks, as shown in Fig. **INSERT FIG.** This design maybe sub-optimal as it does not allow for sub-cooling, as shown in [12]. One degree of freedom, namely the active charge, has been lost to achieve this. We found however that sub-cooling did not add any benefit for this particular system, since the refrigerants are pure and not mixed.

#### DEGREE OF FREEDOM ANALYSIS

As first reported by [12], refrigeration cycles of this kind have five potential steady-state degrees of freedom per closed cycle. These five are the compressor power, the choke valve opening, the active charge and the transferred heat in the condenser and evaporator.

#### Two illustrations: simplified schematic + detailed multi-stream HEX

The model studied in this work is based on the two-stage refrigeration cycle described by [5]. A full description of the model used in this work can be found in [24]. The process is based on a similar refrigeration cycle that is currently being operated in a petrochemical plant. A figure of the process can be seen in Figure 1.

The cycle is a two-stage cycle with two-stage throttling. The two compressor models are based on compressor curves, relating the compressor head, the suction volumetric flowrate and the compressor speed. The compressors are driven by a variable speed steam turbine, which is linked to the compressors with a common drive shaft. For simplicity, it is assumed that no mechanical or thermal heat loss is observed, so that the energy consumption of the compressors equals to the enthalpy difference of the refrigerant from inlet to outlet. Interstage injection of saturated refrigerant increases the energy efficiency by reducing the load in the low pressure evaporator and by reducing the overheat into the second compressor [8]. The injection of saturated vapour can be adjusted by manipulating the control valve  $XV_1$ .

Heat is removed from the system at two different temperatures. The majority of the heat is removed in a kettle reboiler at low pressure (LP) and low temperature. The pressure in this vessel is approximately 1 bar. At intermediate pressure (IP), heat is removed in a flash evaporator at a higher temperature. The pressure in this vessel is around 4 bar. The LP evaporator is approximately ten times larger than the IP evaporator. The distribution of gas and liquid in

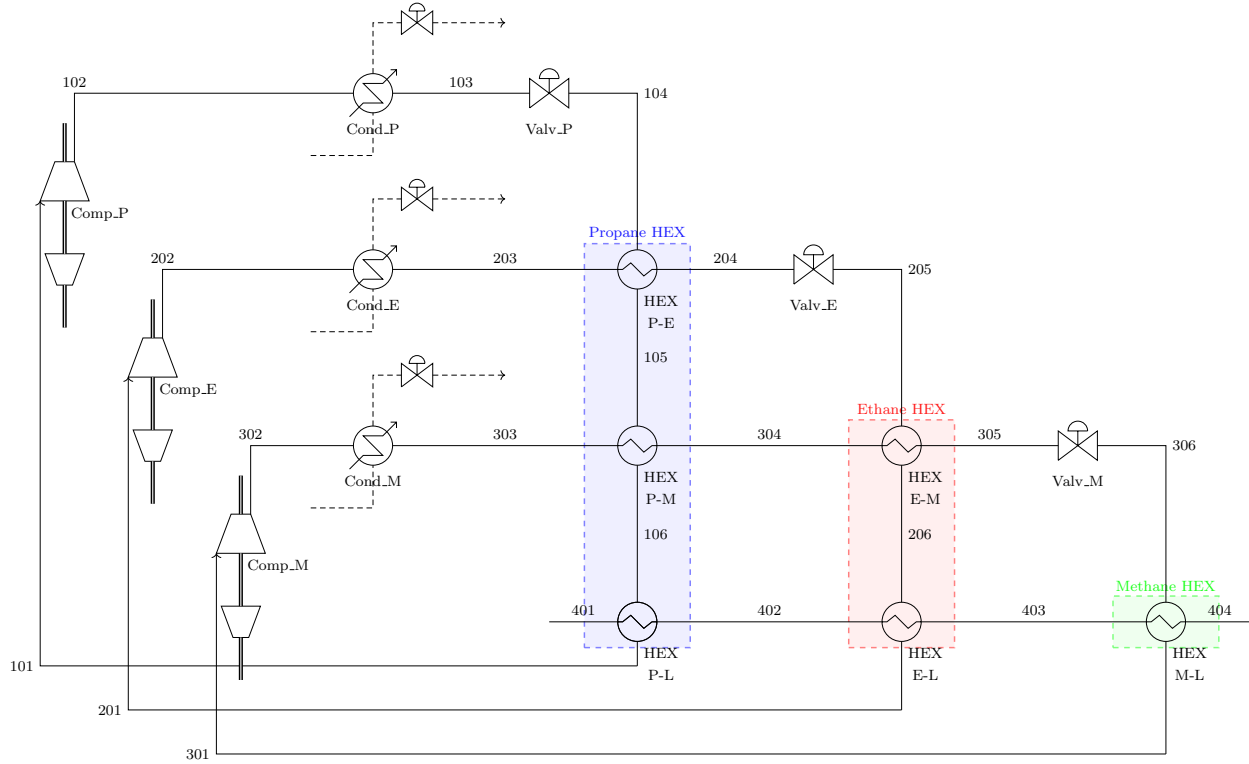


Figure 1: Process flow diagram of the studied process.

the two evaporators can be shifted by adjusting the control valves  $XV_1$  and  $XV_2$ . In both evaporators the process streams exchange heat with the refrigerant through coiled pipes. It is assured that the heating coils are always fully submerged in the liquid by constraining the levels in the tank. The heat transfer coefficient and the heat transfer area are therefore assumed to remain constant at all times.

The compressed refrigerant is condensed in a air-cooled condenser. The condensate is collected in a receiver vessel. The receiver also acts as a buffer tank against disturbances and helps to ensure constant operating conditions in the evaporators and the compressors. Due to the large size of the receiver, it introduces a large capacity to the cycle. This is especially noticable for temperature (and consequently also saturation pressure) measurements, which take a very long time to reach a new steady-state value if a step change in the operating conditions is applied to the system.

The thermodynamic states of the refrigerant are calculated using polynomial approximations of the Helmholtz equations of state calculated by the AllProps software [20].

Due to the recycle loop in the refrigeration cycle, the state derivatives can not

be expressed explicitly, but must be solved iteratively instead. In other words, the process must be written as a DAE system, rather than a ODE system. The model equations from [5] result in a DAE system with six differential equations and ten algebraic equations, though additional equations were added to the system in the current work to accomodate for input dynamics, level controllers and additional algebraic states. The resulting system of equations is integrated with the MATLAB-function `ode15s`.

### 3.2. Defining the optimization problem to find the nominal operating point

The nominal operating point is found by solving an optimization problem where the objective is to minimize the energy consumption of the cycle, subject to operational constraints. The optimization problem is given by

$$\min_{x,u} \quad \phi(x, u, \pi) \quad (10a)$$

$$\text{s.t.} \quad c_E(x, u, \pi) = 0 \quad (10b)$$

$$c_I(x, u, \pi) \leq 0 \quad (10c)$$

$$x_L \leq x \leq x_U \quad (10d)$$

$$u_L \leq u \leq u_U, \quad (10e)$$

where  $x$  signifies the state variables,  $u$  signifies the inputs and  $\pi$  signifies the parameters/disturbances.  $c_E$  and  $c_I$  are the (possibly non-linear) equality and inequality constraints, respectively. Upper and lower bounds on the states and inputs may also be imposed, as seen in (10d) and (10e).

Here, the objective can be expressed as

$$\phi(x, u, \pi) = \sum_i (W_i^{comp.} + \alpha_i m_i^{cond.}), \quad (11)$$

where  $W_i^{comp.}$  is the compressor power of compressor  $i$  and  $m_i^{cond.}$  is the flow rate of air in the condenser. It is common to omit the cost of the condenser from the cost function, in which case the optimal strategy is to cool as much as possible. We consider here the case where fans are used to move the air in the condenser, so we must penalize large air flows as they result in large power consumption from the fans.

The variable  $\alpha$  weights the two terms according to their economic importance. Since prices of raw materials, products and energy are time-variant, it is sensible to consider  $\alpha$  as a disturbance. We could adjust  $\alpha$  through a set-point-generating RTO layer. Alternatively, it is also possible to include measurements of these disturbances in the control structure in a feed-forward fashion. This will be shown in detail later.

The optimization is subject to a number of operational constraints, which are shown in Tab. 1

Table 1: Process constraints and variable bounds for the optimization problem in Eq. (10)

Constraint	Explanation
$T_{404} \leq -150 \text{ }^{\circ}\text{C}$	Maximum LNG outlet temperature
$T_{i03} > T_{ambient}$	Avoid temperature cross in condensers
$0.0 \leq u_{choke,i} \leq 1.0$	Bounds on normalized choke openings
$0.6 \leq u_{comp.,i} \leq 1.1$	Bounds on normalized comp. speeds

### 3.3. Nominal solution

Given the cost function from Eq. (11) and the constraints from Tab. 1, a nonlinear programming problem (NLP) was formulated and implemented in MATLAB using Casadi 3.0.0 [3] and solved using IPOPT 3.12.3 [6].

The nominal solution features one active constraint, namely the upper bound of the LNG outlet temperature constraint. This is somewhat different than the optimal solution reported for a similar MFC process by [11]. They additionally identify active constraints on the super-heating, lower cycle pressures and condenser duties. We have assumed that the degree of super-heating is zero, as this is sub-optimal. We also do not specify a lower pressure constraint, as the pressure is bounded through the efficiency of the compressor in our model. Since we penalize the excessive use of cooling in the condenser to avoid high power consumption, this constraint is not active either.

For each of the refrigeration loops, one liquid inventory must be controlled in accordance with [4]. For this purpose, we chose to use the chokes to control the levels of the low-pressure evaporators. After controlling the levels and the outlet temperature, we are left with 5 degrees of freedom.

It was found that the nominal cost was  $J = 2821 \text{ €/h}$ .

### 3.4. Optimal selection of measurements

Using all available measurements in the calculation of the selection matrix  $\mathbf{H}$  would give the best possible control. However, this is not a viable strategy in practice, since each measurements increases the overall chance of failure of the controller. If the process has not been built, the increased investment cost and complexity of the control structure also advise against the excessive use of measurements. For these reasons, the amount of measurements used in the calculation of  $\mathbf{H}$  should be kept to a minimum. The best subsection of measurements can be determined using the branch and bound algorithm [14]. For the studied process, it was found that five measurements gave acceptably low loss. For the first case, the five best measurements are

$$TC, P_1, TP_1O, FG_1 \text{ and } FG_3$$

### 3.5. Optimality of controlled variables

A self-optimizing controller was implemented with the remaining two unconstrained degrees of freedom. For the five best measurements, the selection



Table 2: Losses for self-optimizing control versus constant setpoint policy for some disturbances. Note that the losses are very small compared to the nominal cost of  $J = 2831 \text{ €/h}$

Variable	Disturbance	Loss [€/h]	
		Self-optimizing	Constant inputs
$TP_1I$	+3K	$0.340 \cdot 10^{-2}$	$15.114 \cdot 10^{-2}$
$TP_2I$	+3K	$0.076 \cdot 10^{-2}$	$0.018 \cdot 10^{-2}$
$TP_3I$	+3K	$0.020 \cdot 10^{-2}$	$3.424 \cdot 10^{-2}$
$FCP_1$	+10W K <sup>-1</sup>	$17.146 \cdot 10^{-2}$	$29.366 \cdot 10^{-2}$
$FCP_2$	+3W K <sup>-1</sup>	$0.190 \cdot 10^{-2}$	$0.208 \cdot 10^{-2}$

matrix  $\mathbf{H}$  was calculated using Equation 9. The variance matrix  $\mathbf{W}_{\mathbf{ny}}$  was constructed assuming that the variance of each measurement is equal to 1% of the nominal value. For temperature measurements,  $\omega_{T_i} = 0.5 \text{ K}$  was used. The expected disturbances were assumed to include  $TP_1I$ ,  $TP_2I$  and  $TP_3I$ , being the inlet temperatures to the LP evaporator, the inlet temperature to the IP evaporator and the inlet temperature of the air in the condenser, respectively.  $FCP_1$  and  $FCP_2$ , being the combined mass flow rate and heat capacity of the process inlet to the LP and IP evaporators respectively, were also treated as disturbances. The variances of the disturbances were set to  $\sigma_{TP_1I} = 3 \text{ K}$ ,  $\sigma_{TP_2I} = 3 \text{ K}$ ,  $\sigma_{TP_3I} = 5 \text{ K}$ ,  $\sigma_{FCP_1} = 10 \text{ W/K}$  and  $\sigma_{FCP_2} = 3 \text{ W/K}$ .

The performance of the controller was tested for a set of disturbances as shown in Table 2. The steady-state losses are compared to the losses from a constant-input policy. It can be seen that the closed-loop loss is significantly lower than the open-loop loss on average. However, for some disturbances the losses are in fact higher for the controlled system. This is to be expected when using the formulation from Equation 4. Even though the effect of implementation error is not shown here, it can be observed that the closed-loop system outperforms the open-loop system.

It is also observed that the losses are almost negligible compared to the nominal values of the cost function. Indeed, simulations revealed that the cost function was very flat around the nominal point. This is desirable according to [22], since the effect of implementation errors is minimized. In the same vein, it is desirable that the optimum value of  $\mathbf{c}$  is insensitive to disturbances to avoid losses from keeping  $\mathbf{c}$  constant. Figure 2 shows the location of the optimal values of  $\mathbf{c}$  relative to the nominal setpoint. As can be seen when comparing Figure 2 to for instance the magnitude of the open-loop change in  $\mathbf{c}$  due to a disturbance as seen in Figure 3, it is safe to say that the optimal value of  $\mathbf{c}$  is independent to disturbances. The resulting losses from disturbances are therefore expected to be small.

All disturbances except the disturbance in the flow rate into the LP evaporator,  $FCP_1$ , are located on the line going through a valley-shaped minimum of the cost surface. This is the principle eigenvector of the elliptic hyperboloid. This explains why the loss associated with disturbing  $FCP_1$  is an order of mag-

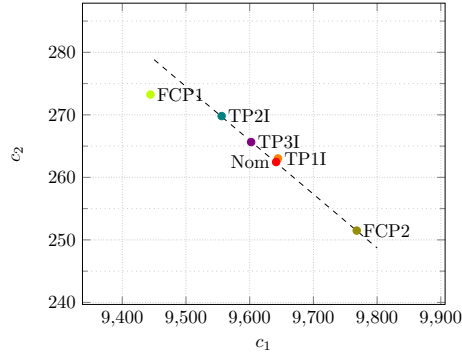


Figure 2: Optimal values of  $\mathbf{c}$  for the studied disturbances. We observe that the optimal values of  $\mathbf{c}$  for the disturbances are grouped very closely around the nominal point. Notice the scale of the axis compared to i.e. the open-loop changes in  $\mathbf{c}$  to a disturbance in Figure 3.

nitude larger than for the other disturbances. It is also observed that the losses due to the two disturbances associated with the IP evaporator, that is  $TP_2I$  and  $FCP_2$ , are smaller than the corresponding losses caused by disturbances of the LP evaporator. This is caused by the fact that  $p_{TP_1O} > p_{TP_2O}$  in Equation 11.

### 3.6. Dynamic simulation

The derived self-optimizing controller was implemented into the dynamic system by introducing two PID controllers. It was chosen to pair the compressor speed  $N$  with  $c_1$  and the valve opening  $XV_1$  with  $c_2$ . The PID tunings were derived based on the SIMC rules [23]. As can be seen from Figure 3, the resulting PID controller has a somewhat large time constant. The controller can be tuned more aggressively by choosing a smaller closed-loop time constant, at the cost of robustness.

The dynamic performance of the self-optimizing controller was tested by applying a step in the inlet temperature to the LP evaporator,  $TP_1I$ . It was found that the responses of the open-loop and the closed-loop systems were almost identical, as can be seen in Figure 3. The integrated error for the closed loop system is smaller than for the open loop, but the difference is marginal.

It is noted that the open-loop response pushes the states along the dashed line in Figure 2 corresponding to the minimum valley of the cost surface in the  $\mathbf{c}$ -space. Even though the observed open-loop response pushes the states north-east, away from the optimal point (marked orange in Figure 2), the location at the bottom of the valley still ensures very low losses.

From Figure 3 it can be seen that it takes a relatively long time for the loss to stabilize after it has been disturbed, even though the controlled variable reaches its setpoint almost immediately. This behaviour is due to the slow dynamics of the system. The slow dynamics are caused by the large capacity of the HP receiver, and is an inherent property of the system that can not be circumvented with feedback control.

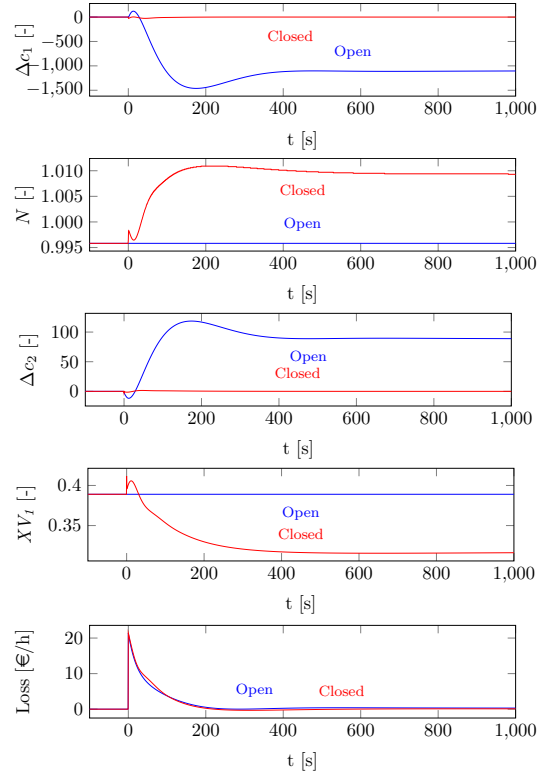


Figure 3: Case 1: Response of the controlled variables ( $\Delta c_1$  and  $\Delta c_2$ ) and the manipulated variables ( $N$  and  $XV_1$ ) to a  $-3K$  step in  $TP_I I$  for open loop and closed loop. The final plot compares the loss for the open loop and the closed loop.

Slow dynamics aside, it seems as if the process is so rigid in its design and parametrization that the cost function is characterized by an almost flat surface. This means that the process will be close to optimal even when in an open-loop configuration. It does therefore not make a significant difference if the system is controlled to optimality directly or if the unconstrained degrees of freedom are used to control other CVs. By controlling for example the evaporator pressures or the outlet temperatures directly, one can achieve tighter product specifications on the process side, at only minimal cost impact.

#### 4. Case two - Including measurements of economic parameters

A second case was simulated to study the possibility of including measurements of the cost parameters  $p_W$ ,  $p_{TP_1O}$  and  $p_{TP_2O}$  in the setpoint of the self-optimizing controller.

The same process model and cost function as previously discussed in Section 3.1 is being used, so the optimal steady-state solution is the same as for the first case.

##### 4.1. Self-optimizing control

Instead of treating the parameters  $p_W$ ,  $p_{TP_1O}$  and  $p_{TP_2O}$  in the cost function as static parameters, it was decided to include measurements of these parameters in the construction of the selectivity matrix  $\mathbf{H}$ . This way, the controller can react to changes in the power prices and the prices of the products immediately, without being dependent on an overlying real-time optimization layer. A similar controller is discussed by [10]. The controller will give optimal operation of the plant as long as the market only has random price fluctuations. Due to the linearization around the nominal point, the self-optimizing controller is only optimal locally. Whenever prices start to change permanently, the controller must be re-parameterized.

It was assumed that the measurements of  $p_W$ ,  $p_{TP_1O}$  and  $p_{TP_2O}$  are noiseless, meaning that there is no measurement error on these measurements. This assumption was made since the information about the economic parameters is not contained in the states of the system, therefore it is not possible to decrease any uncertainty related to these measurements by linear combinations of the outputs. Since the measurements of  $p_W$  and  $p_{TP_1O}$  are not prone to instrumentation error like i.e. pressure or temperature meters, this assumption seems reasonable.

The best subset of measurements was again found using the branch and bound algorithm. It was found that the best subset of eight measurements includes

$$XV_1, P_1, P_2, TP_1O, FL_2, FL_4, p_W \text{ and } p_{TP_1O}$$

It can be seen that the branch and bound algorithm does not give a set of measurements including all three economic parameters.  $p_{TP_2O}$  is not included

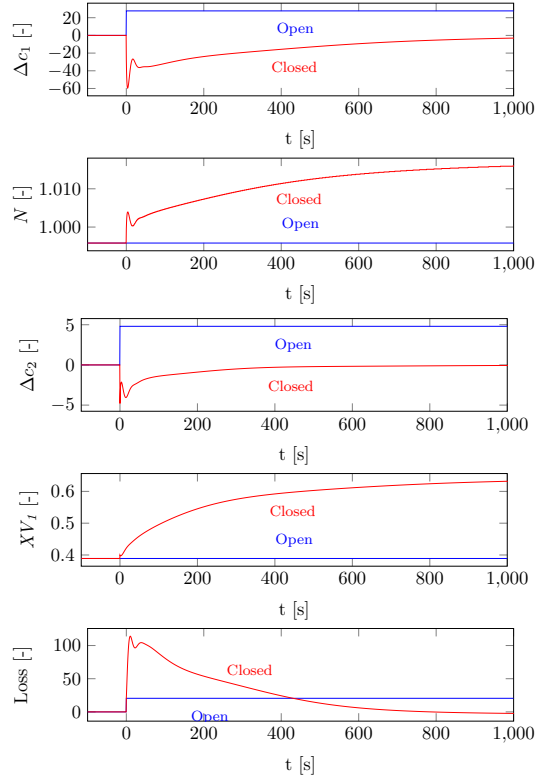


Figure 4: Case 2: Response of the controlled variables ( $\Delta c_1$  and  $\Delta c_2$ ) and the manipulated variables ( $N$  and  $XV_I$ ) to a step in  $p_W$  for open loop and closed loop. The final plot compares the loss in the cost function for the open loop and the closed loop.

because the expected loss is very small. Consequently the controller will not be able to react to changes in the price of the process stream in the IP evaporator.

The selection matrix  $\mathbf{H}$  and the corresponding set-point  $\mathbf{c}$  is calculated from Equation 9.

The closed loop response to a +10% step in the energy price  $p_W$  is shown in Figure 4.

The derived controller is able to react to changes in the economic parameters. Again, it is observed that the slow dynamics of the system cause the loss of the controller to very slowly reach a new steady state value. After approximately 400 seconds the closed-loop self-optimizing controller starts outperforming the open-loop controller.

## 5. Conclusion

In this paper we have investigated the possibilities of applying self-optimizing control to a two-stage refrigeration cycle. Since the cost function is formulated to

give a trade-off between energy consumption and evaporator outlet temperature, it was found that the optimal point of operation leaves the compressor speed  $N$  unconstrained. In addition, it was found that the valve opening  $XV_I$  remained unconstrained. Using the two degrees of freedom, a self-optimizing controller was implemented.

It was found that the self-optimizing controller does decrease the deviation from optimal operating conditions when disturbed. However, the decrease in observed loss is relatively small, mainly due to the flatness of the cost surface. This means that self-optimizing control is not strictly necessary to decrease the average loss to acceptable levels, as the system is already nearly optimal to begin with. Most likely, the observed behaviour is a feature of the studied model and model parameterization only. Other refrigeration cycles could benefit more from having self-optimizing control implemented.

It was shown that self-optimizing control is relatively fast and easy to implement, so that self-optimizing control can be considered a viable alternative to model-based control systems. This particular system would probably benefit from model-based control system due to the slow dynamics. A smaller cycle with lower capacity could probably be kept sufficiently optimal with self-optimizing control only. More work needs to be done to compare the advantages and disadvantages of the different control approaches for multi-stage refrigeration cycles.

It was also shown that self-optimizing control can include economic measurements to maintain optimal operation under price fluctuations. This lessens the need for supervisory real-time optimization.

- [1] Alstad, V. and Skogestad, S. (2007). Null space method for selecting optimal measurement combinations as controlled variables. *Industrial & engineering chemistry research*, 46(3), 846–853.
- [2] Alstad, V., Skogestad, S., and Hori, E.S. (2009). Optimal measurement combinations as controlled variables. *Journal of Process Control*, 19(1), 138–148.
- [3] Andersson, J. (2013). *A General-Purpose Software Framework for Dynamic Optimization*. PhD thesis, Arenberg Doctoral School, KU Leuven, Department of Electrical Engineering (ESAT/SCD) and Optimization in Engineering Center, Kasteelpark Arenberg 10, 3001-Heverlee, Belgium.
- [4] Aske, E.M.B. and Skogestad, S. (2009). Consistent inventory control. *Industrial & engineering chemistry research*, 48(24), 10892–10902.
- [5] Asmar, B.N. (1991). *Control of a two-stage refrigeration cycle*. Ph.D. thesis, University of Nottingham - School of Chemical, Environmental and Mining Engineering.
- [6] Biegler, L.T. (2010). *Nonlinear programming: concepts, algorithms, and applications to chemical processes*, volume 10. SIAM.

- [7] Ellis, M., Durand, H., and Christofides, P.D. (2014). A tutorial review of economic model predictive control methods. *Journal of Process Control*, 24(8), 1156 – 1178. Economic nonlinear model predictive control.
- [8] Granryd, E. (2009). *Refrigerating engineering*. Royal Institute of Technology, KTH, Department of Energy Technology, Division of Applied Thermodynamics and Refrigeration.
- [9] Hovgaard, T.G., Larsen, L.F., Edlund, K., and Jørgensen, J.B. (2012). Model predictive control technologies for efficient and flexible power consumption in refrigeration systems. *Energy*, 44(1), 105–116.
- [10] Jäschke, J. and Skogestad, S. (2011). Optimal operation by controlling the gradient to zero. In *Proc. of 18th IFAC World Congress*, 6073–6078. IFAC.
- [11] Jensen, J.B. and Skogestad, S. (2006). Optimal operation of a mixed fluid cascade lng plant. *Computer Aided Chemical Engineering*, 21, 1569–1574.
- [12] Jensen, J.B. and Skogestad, S. (2007). Optimal operation of simple refrigeration cycles: part i: degrees of freedom and optimality of sub-cooling. *Computers & chemical engineering*, 31(5), 712–721.
- [13] Jensen, J.B. and Skogestad, S. (2007). Optimal operation of simple refrigeration cycles: part ii: selection of controlled variables. *Computers & Chemical Engineering*, 31(12), 1590–1601.
- [14] Kariwala, V. and Cao, Y. (2009). Bidirectional branch and bound for controlled variable selection. part ii: Exact local method for self-optimizing control. *Computers & Chemical Engineering*, 33(8), 1402 – 1412.
- [15] Kariwala, V., Cao, Y., and Janardhanan, S. (2008). Local self-optimizing control with average loss minimization. *Industrial & Engineering Chemistry Research*, 47(4), 1150–1158.
- [16] Larsen, L.F.S. (2006). *Model based control of refrigeration systems*. Ph.D. thesis, Aalborg University.
- [17] Larsen, L.F., Izadi-Zamanabadi, R., and Wisniewski, R. (2007). Supermarket refrigeration system-benchmark for hybrid system control. In *Proc. of ECC07*.
- [18] Larsen, L.S., Thybo, C., Stoustrup, J., and Rasmussen, H. (2003). Control methods utilizing energy optimizing schemes in refrigeration systems. In *Proc. of ECC2003*.
- [19] Leducq, D., Guilpart, J., and Trystram, G. (2006). Non-linear predictive control of a vapour compression cycle. *International journal of Refrigeration*, 29(5), 761–772.

- [20] Lemmon, E., Jacobsen, R., Penoncello, S., and Beyerlein, S. (1994). Computer programs for the calculation of thermodynamic properties of cryogenics and other fluids. In P. Kittel (ed.), *Advances in Cryogenic Engineering*, volume 39 of *Advances in Cryogenic Engineering*, 1891–1897. Springer US.
- [21] Sarabia, D., Capraro, F., Larsen, L.F., and De Prada, C. (2007). Hybrid control of a supermarket refrigeration systems. In *Proc. of American Control Conference*, 4178–4185. IEEE.
- [22] Skogestad, S. (2000). Plantwide control: the search for the self-optimizing control structure. *Journal of Process Control*, 10(5), 487 – 507.
- [23] Skogestad, S. (2003). Simple analytic rules for model reduction and pid controller tuning. *Journal of Process Control*, 13(4), 291 – 309.
- [24] Verheyleweghen, A. (2015). *Modelling and Simulation of a Two-Stage Refrigeration Cycle*. Master’s thesis, Norwegian University of Science and Technology.
- [25] Wright, S.J. and Nocedal, J. (1999). *Numerical optimization*, volume 2. Springer New York.
- [26] Yelchuru, R. and Skogestad, S. (2010). Miqp formulation for optimal controlled variable selection in self optimizing control. *PSE Asia*, 25–28.